JGR Atmospheres

RESEARCH ARTICLE
10.1029/2019JD031488

Daytime Variability of Cloud Fraction From DSCOVR/EPIC Observations

A. Delgado-Bonal[1,2], A. Marshak[1], Y. Yang[1], and L. Oreopoulos[1]

[1]Earth Sciences Division, NASA Goddard Space Flight Center, Greenbelt, MD, USA, [2]Universities Space Research Association, Columbia, MD, USA

Abstract The location of the Earth Polychromatic Imaging Camera (EPIC) aboard the Deep Space Climate Observatory (DSCOVR) offers a global view of the Earth and captures its atmosphere at different locations and time of the day. In this paper, we take advantage of that unique feature to study the daytime variability of cloud fraction in a seasonal and zonal context. We observe that the ensemble behavior over ocean has a distinctive convex shape, with higher cloud fractions at early morning and late afternoon, while no such pattern is seen over land. Unique perspectives are obtained by analyzing the cloud fraction of the globe as a whole and separately for each hemisphere, and by studying the effect of the viewing zenith angle on cloud fraction retrievals.

Plain Language Summary Images from the Earth Polychromatic Imaging Camera instrument aboard the Deep Space Climate Observatory satellite are unique compared to those from other satellites since the left edge of the image corresponds to sunrise, the right edge to sunset, and the middle to noon. That capability of capturing different parts of the day in a single picture allows us to study the daytime behavior of cloud fraction in new ways. When conducting separate analysis over ocean and land, we find that cloud fraction over ocean is generally higher in the early morning and late afternoon and minimum during the central hours of the day. However, the behavior over land is generally flat with only a very slight increase in the afternoon.

Key Points:
- EPIC observes the sunlit side of the Earth with a frequency between 1 and 2 hr providing information on cloudiness at different local times
- Four years of EPIC global cloud fraction was analyzed as a function of season and latitude
- The daytime evolution of cloudiness over ocean exhibits a clear convex shape, while it has less pronounced features over land

Supporting Information:
- Supporting Information S1

Correspondence to:
A. Delgado-Bonal,
alfonso.delgadobonal@nasa.gov

Citation:
Delgado-Bonal, A., Marshak, A., Yang, Y., & Oreopoulos, L. (2020). Daytime variability of cloud fraction from DSCOVR/EPIC observations. *Journal of Geophysical Research: Atmospheres*, *125*, e2019JD031488. https://doi.org/10.1029/2019JD031488

Received 6 AUG 2019
Accepted 17 APR 2020
Accepted article online 26 APR 2020

1. Introduction

The Earth Polychromatic Imaging Camera (EPIC) aboard the Deep Space Climate Observatory (DSCOVR) captures the sunlit side of Earth with a frequency between roughly 1 hr (during Northern Hemisphere summer) and 2 hr (during Northern Hemisphere winter). Unlike geostationary satellites, DSCOVR observes the Earth from the L1 Lagrangian point approximately 1.5×10^6 km away, observing the state of the atmosphere and surface from sunrise to sunset in the same image. Therefore, a single image from EPIC provides information about cloudiness at different hours of the day, offering information from early morning (left side of the image) to late afternoon (right side of the image).

With EPIC, for the first time, global daytime cloud variability can be analyzed using observations from a single sensor. Even though similar analysis can also be done with multisensor composite data sets such as the one from the International Satellite Cloud Climatology Project (ISCCP) (Rossow & Schiffer, 1991; Young et al., 2018), using EPIC data helps avoid cross-sensor calibration and consistency issues; hence, more robust results can be expected.

Daytime cloudiness is one of the determining factors of the Earth's planetary albedo. Understanding its variability is important to the climate system modeling. Comparison of diurnal cloud fraction cycles in GCMs and reanalysis data sets such as the European Centre for Medium-Range Weather Forecasts twentieth century reanalysis (e.g., Yin & Porporato, 2017) shows that each of those data sets provides slightly different characteristics for the daytime cycle. To reduce diurnal cloud cycle biases in climate models, this paper provides direct observations of the daytime variability of cloud fraction based only on the statistics of 4 years of EPIC images.

Since EPIC images are georectified, the determination of local time is simply carried out for each pixel using the longitude information field and the Universal Time Coordinated (UTC) of the data set. One can thus obtain information about cloud fraction between 6 a.m. and 6 p.m. in each image. In contrast,

instruments on sun-synchronized satellites, such as MODIS, provide a single daytime image of most locations at a specific time of the day, which is insufficient for analyzing the daily behavior (Platnick et al., 2017). Furthermore, when different satellites are used to monitor cloud fraction such as in the case of Terra and Aqua, the exact offset between the satellites varies with the latitude, and those changes in local time should be considered when data are combined to estimate the diurnal cycle (Levy et al., 2018; Loeb & Doelling, 2020).

The spectral range captured by EPIC covers ultraviolet (318, 325, 340, and 388 nm), visible (443, 551, 680, and 688 nm), and near infrared (764 and 780 nm). Although the instrument does not have thermal infrared sensors and therefore relevant spectral tests, such as temperature contrast for cloud detection, cannot be performed, alternate methodologies have been developed to determine the cloud mask (Yang et al., 2019). However, as the algorithms are different, differences in the ability to detect clouds when compared with other instruments are expected.

EPIC is equipped with a 2,048 × 2,048 pixel charge-coupled device (CCD) array, and its resolution depends on viewing zenith angle (VZA). The best resolution of the image is at nadir where the viewing (and solar) zenith angle is close to 0°, with a pixel size of approximately 8 km. When the VZA increases, resolution coarsens as the longer axis of the pixel increases as $\cos^{-1}$(VZA), while the shorter axis remains unchanged. In our analysis we weigh all pixels equally. Therefore, the variation of the VZA could affect the results and has to be analyzed in detail, as we will see later.

This paper is structured as follows. In section 2 we describe the data and methodology used in our analysis, while in section 4 we present the main results by compositing for different situations. First, we investigate cloud behavior over ocean compared to land and study the daytime evolution for both cases separately providing a spatial (latitude) and temporal (daytime) analysis for the latitudes from 60°S to 60°N. To illustrate more clearly the daytime behavior and the differences between land and ocean, we also show the results of the analysis separately for the Northern and Southern Hemispheres. Finally, we investigate the effect of the VZA in the analysis to examine the sensitivity of the results and quantify the importance of the larger pixels. In addition to the global Earth, four regional analyses of marine stratocumulus and convective clouds over land are provided in the supporting information.

2. Data and Methods

This study is based on the EPIC's cloud fraction retrievals as part of the Level 2 EPIC cloud products, currently a collection of approximately 16,500 granules starting from June 2015. The EPIC cloud products are described in detail in Yang et al. (2019), while EPIC calibration of the visible and near IR channels is reported in Geogdzhayev and Marshak (2018).

For each pixel, EPIC cloud products contain different information including latitude, longitude, solar zenith angle (SZA), and cloud mask. The cloud mask labels each pixel with a different number ranging between 1 and 4, classifying it as clear with high confidence (1), clear with low confidence (2), cloudy with low confidence (3), or cloudy with high confidence (4). Previous analyses of EPIC granules have shown that the cloud mask matches well the RGB images, obtaining values for the global cloud fraction of each full-disc image of ~65%. The EPIC cloud fractions have also been compared with those from geosynchronous and low Earth orbit satellites showing differences of only 1.5% in the global cloud fraction estimates compared to GEO-LEO composite data sets (Yang et al., 2019).

For our analysis, we scan each EPIC granule and determine the local time for each pixel using the UTC time of the EPIC image and the longitude associated to each pixel. We also divide the latitudes from 60°S to 60°N into bins of 5° and stratify pixels using the latitude field included in the granule. We then aggregate the seasonal values in 24-hourly intervals; for example, any pixel with local time from 10:00 to 11:00 a.m. is assigned in that hourly interval. For each hourly interval, we count the number of pixels with cloud mask equal to 3 and 4, as well as the total number of pixels for that interval. Once the granules of the whole season have been scanned, the cloud fraction is calculated for each hourly interval as a simple average of the number of pixels with cloud mask equal to 3 or 4, divided by the total number of pixels for that hour. Note that the number of pixels with cloud mask equal to 3 corresponds to less than 1.5% of all the pixels in the latitudes from 60°S to 60°N.

The above procedure was used to analyze all available granules from June 2015 to June 2019, obtaining the cloud fraction hourly values for each of the 4 years and for each season: December-January-February (DJF 2015/2016, 2016/2017, 2017/2018, and 2018/2019), March-April-May (MAM 2016, 2017, 2018, and 2019), June-July-August (JJA 2015, 2016, 2017, and 2018), and September-October-November (SON 2015, 2016, 2017, and 2018). Finally, we calculate an equal-weight average of the 4 years for each season to provide cloud fraction in a temporal (hourly) and spatial (latitude) way.

Since cloud climatology is known to be different over land and over ocean, we follow the common practice of separating the analysis depending on surface type. For that purpose, we use the International Satellite Land Surface Climatology Project-Initiative II Data Collection binary classification file with a quarter degree resolution (ISLSCP, 2013). The daily cycle of cloud fraction is paramount for correct estimates of the Earth's energy budget, and diurnal biases in current climate models can result in inaccurate warming or cooling cloud effects on hourly and daily scales, particularly over land (Yin & Porporato, 2017). In radiative flux comparisons between observations and models, the distinction between land and ocean is crucial as climate models show substantial differences in the individual components of the energy budget between the two (Wild et al., 2015). Since clouds play a major role in the energy budget, separate analysis over land and ocean to highlight differences in daily cycles on global scales makes sense.

With the above in mind, our section 3 analysis is structured as follows. Section 3.1 shows the latitudinal analysis for different seasons, while section 3.2 separates the analysis between Northern and Southern Hemispheres as a way to emphasize the diurnal cycle differences between land and ocean. Finally, section 3.3 evaluates the impact of the VZA on the results. Since we are performing a global analysis, we are mixing pixels with different VZAs. For EPIC, the VZA and SZA are essentially the same so we study three different situations: (i) all pixels, (ii) pixels with SZA $< 78°$, and (iii) pixels with SZA $< 60°$.

3. Results

EPIC captures the sunlit side of the Earth from sunrise (left edge) to sunset (right edge), as shown in Figure 1 (left panels). The current L2 cloud product includes the GPS geolocation information of each pixel which allows us to determine the corresponding location in a grid such as the one of the right panels and thus the local hour of each pixel.

3.1. Latitudinal Analysis of cloud Fraction Over Ocean and Land

In this section, we evaluate the cloud fraction using all pixels captured by EPIC from June 2015 to June 2019, after classifying the pixels as ocean or land with a quarter degree resolution and aggregating the data in 5° latitude zones on an hourly basis for the four different seasons. Figure 2 shows the average cloud fraction (bottom) and the number of pixels analyzed (top) for five different time intervals for all seasons. Note that the hours around noon (red and blue lines) correspond to the center of the image and therefore contain more pixels than early morning or late afternoon.

After cloud fraction for all individual hours has been calculated, we determine the daytime average (black line) as the simple average of all hours from 6 a.m. to 6 p.m. The time periods with low pixel number are not accounted for in the calculation of the daytime averages. We specified a threshold value of 10% of the maximum number of pixels of the season and disregarded the hours that do not pass this threshold to calculate the daytime average. We shadowed that range in the top of Figure 2 and dashed the lines that fall into that area in the bottom of Figure 2. For example, for the time interval from 5 p.m. to 6 p.m. in DJF (purple line), for latitudes below 0° (Southern Hemisphere), the number of pixels is above 10%, and therefore, it is considered statistically significant to be included in the daytime average. However, for latitudes above 0° (Northern Hemisphere), the number of pixels decreases drastically and it is not accounted for in the daytime average.

Figure 2 shows the results of this analysis over ocean, where a particular behavior is observed for all four seasons: The cloud fraction is higher in the morning, decreases toward noon, and increases again in the afternoon, which results in a convex shape if plotted against time as will be shown in latter discussion (positive second derivative). Interestingly, this pattern is repeated throughout all latitudes over ocean (see the order of colored curves) and EPIC provides an unprecedented opportunity to study it further.

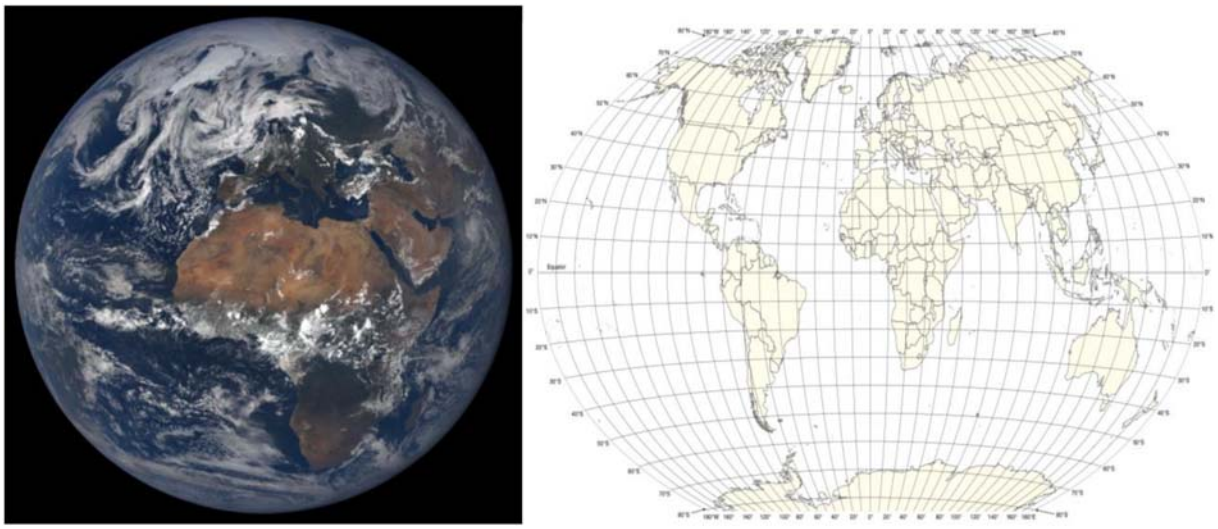

Figure 1. Left panels: EPIC image taken on 13 June 2019 around noon UTC. Right panels: Winkel tripel projection of the Earth over a longitudinal and latitudinal grid of 10° × 10°.

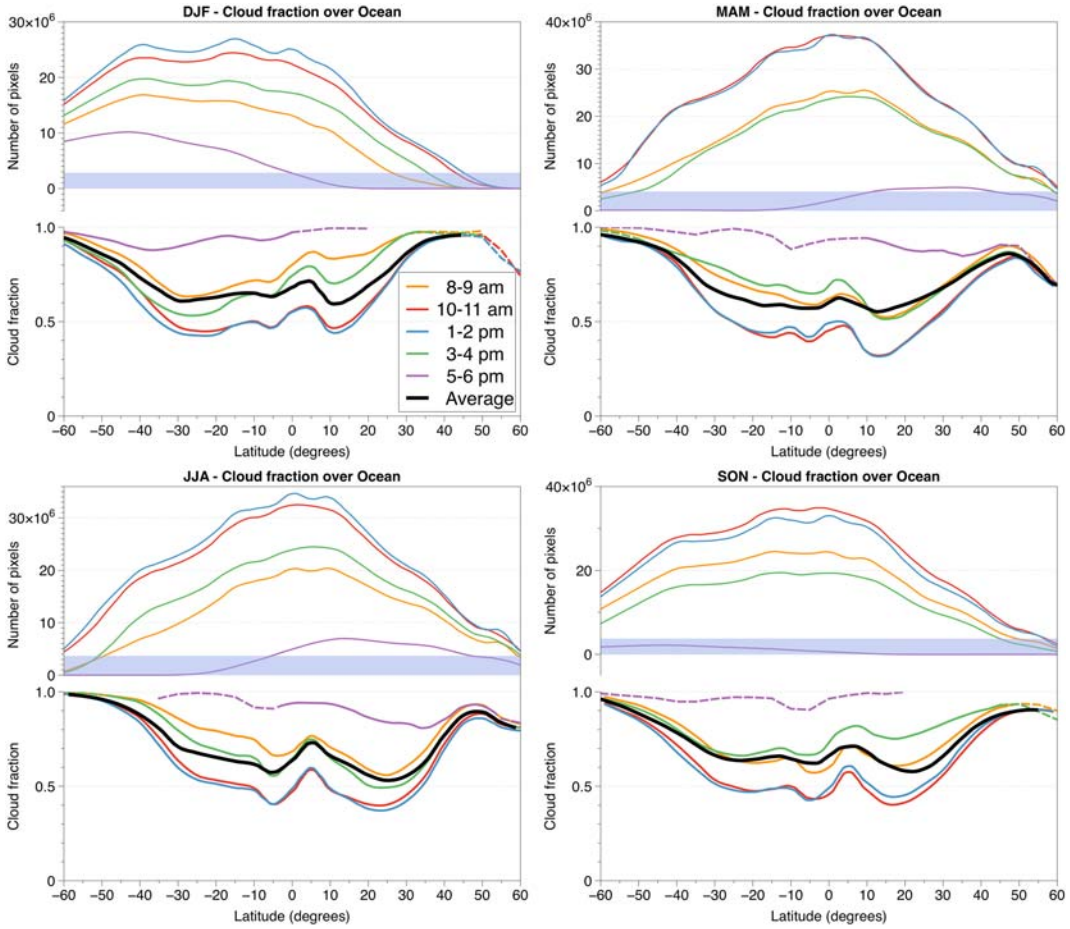

Figure 2. Cloud fraction over ocean versus latitude for four seasons. Top panels: number of pixels analyzed for different local time intervals. The shadowed area corresponds to the lower 10% of the maximum number of pixels each season. Bottom panels: cloud fraction for five different time intervals. The dashed lines represent the hours and latitudes for which the fraction of pixels is below 10%. The daytime average (black line) does not include latitudes where sampling falls below the 10% threshold (i.e., the dashed portion of the lines).

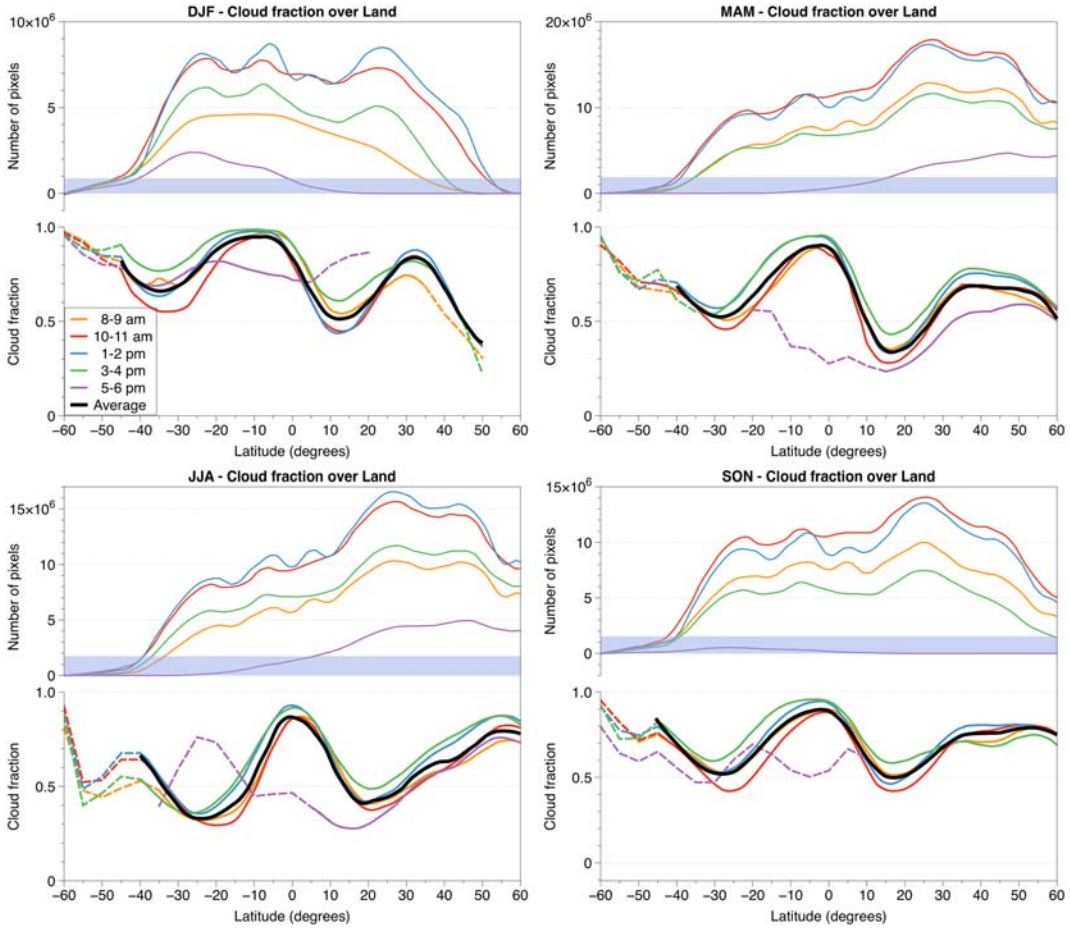

Figure 3. As in Figure 2 but for land.

Figure 3 provides a similar analyis for clouds over land. As in the previous figure, we show the analyzed number of pixels for each time interval versus latitude (top) and the average cloud fraction for each time interval (bottom). Similarly, the shadowed area in the top of the figure corresponds to the 10% of pixels sampling threshold which has to be exceeded for inclusion in the daytime average calculation (black lines).

We observe several differences over land compared to ocean. First, we notice that the cloud fraction for the different hours is much closer to the daytime average, indicating less variability during day time. Second, we observe that there is no distinguishable pattern in the hourly behavior that is common for all the seasons. Finally, as the number of pixels is smaller, the behavior at late afternoon is more erratic and its contribution to the daytime mean depends on the latitude.

As stated earlier, EPIC captures all latitudes and longitudes of the sunlit side of the Earth at the same time. On the other hand, images from sun synchronized satellites depend on the orbit and the latitude, capturing the state of the atmosphere at specific hours of the day. Furthermore, even though the equator crossing time for Terra and Aqua is at 10:30 a.m. and 1:30 p.m., the actually local time of observation still depends on the location (Levy et al., 2018) and multiple acquisitions per day are possible at high latitudes because of orbit overlap. Those facts should be considered when drawing comparisons with the present work.

Our results can be compared with previous results such as those in King et al. (2013). These authors show the zonal mean daytime cloud fraction over land and ocean derived from Terra (2000–2011) and Aqua (2002–2011) for all seasons. It can be seen that, in general, our results match the shape and latitudinal behavior in that investigation. The values of cloud fraction over ocean range from approximately 0.6 to 1.0, similar to our reported daytime average (black lines), with the values varying with latitude in a similar fashion,

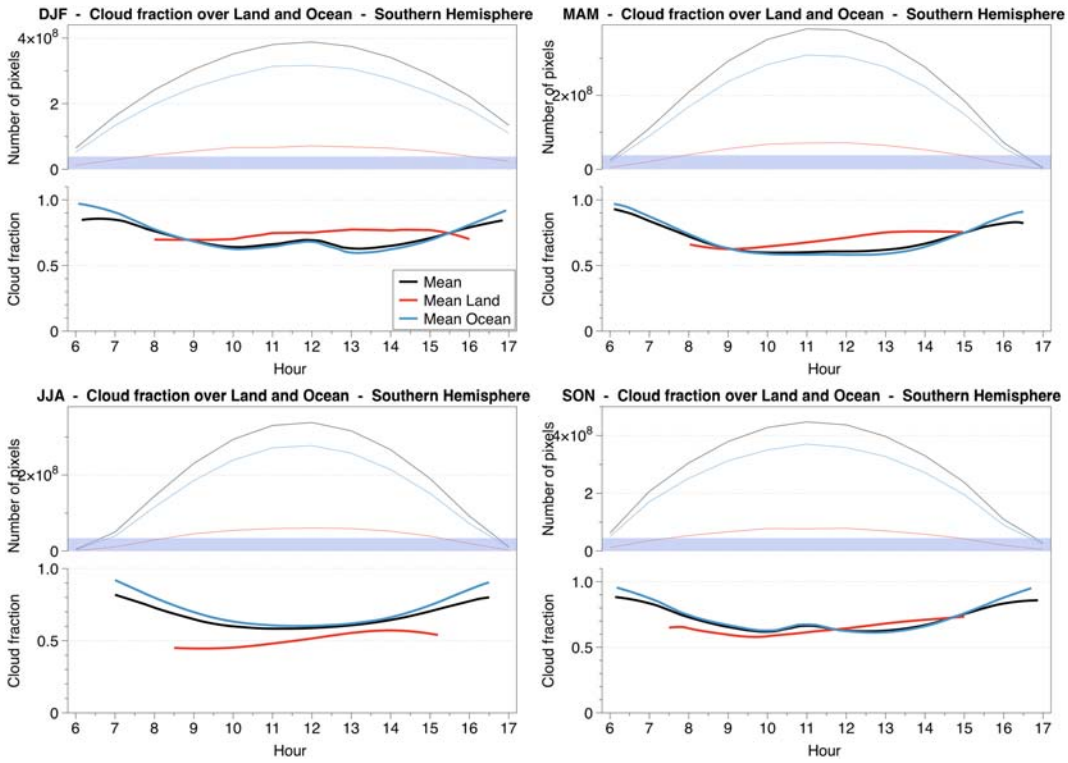

Figure 4. Cloud fraction separately over land and ocean and combined versus local time of the day for the Southern Hemisphere.

being almost 1.0 for 60°S and 60°N over ocean. However, our reported values for the corresponding times of Terra (10:30 a.m.) and Aqua (1:30 p.m.) do not match exactly cloud fractions in Figure 4 of King et al. (2013), being lower than the daytime average, with values as low as 40% at certain latitudes. In contrast, at other times, the cloud fraction for these latitudes is above the daytime mean, showing the strong diurnal cycle of the cloud fraction for some latitudes which GEO-LEO satellites are unable to capture.

These features underline the added value of EPIC, showing that cloud fraction varies during the day. Previous investigations based on ISCCP have probed the daily behavior of clouds (Kondragunta & Gruber, 1994) and decomposed into low, middle, and high clouds (Bergman & Salby, 1996; Cairns, 1995; Yin & Porporato, 2017). In our research, which does not distinguish cloud fraction by height category, we obtain a similar convex pattern as previously reported over ocean with ISCCP and a more constant cloud fraction over land due to the combination of high clouds (convex pattern during day time) and low clouds (concave pattern during day time) (Bergman & Salby, 1996). One should keep in mind that the frequency sampling in ISCCP analyses is 3 hr, and the whole Earth, including nighttime, is covered by a constellation of satellites, while EPIC data sets have a frequency of 1 or 2 hr and capture only the sunlit side of the Earth.

3.2. Hourly Variation of Cloud Fraction

Next, we investigate here the hourly behavior for the Southern and Northern Hemispheres to illustrate the differences between land and ocean. As explained earlier, this distinction is motivated by studies related to the energy balance of the planet. The predictions carried out with GCMs have different types of biases over land and ocean in the calculation of the daily cycle of cloud fraction. Those discrepancies may influence the land-ocean-atmosphere interaction of the model and have a significant impact on the climate projections. Thus, we use EPIC to properly characterize the differences in the daytime cycles over land and ocean for both hermispheres.

As an example, Figure 4 shows the hourly behavior of cloud fraction over ocean and over land for the Southern Hemisphere, along with the number of pixels and their corresponding 10% threshold shadowed area. It is remarkable that the behavior over ocean shows a clear convex function with changes of almost

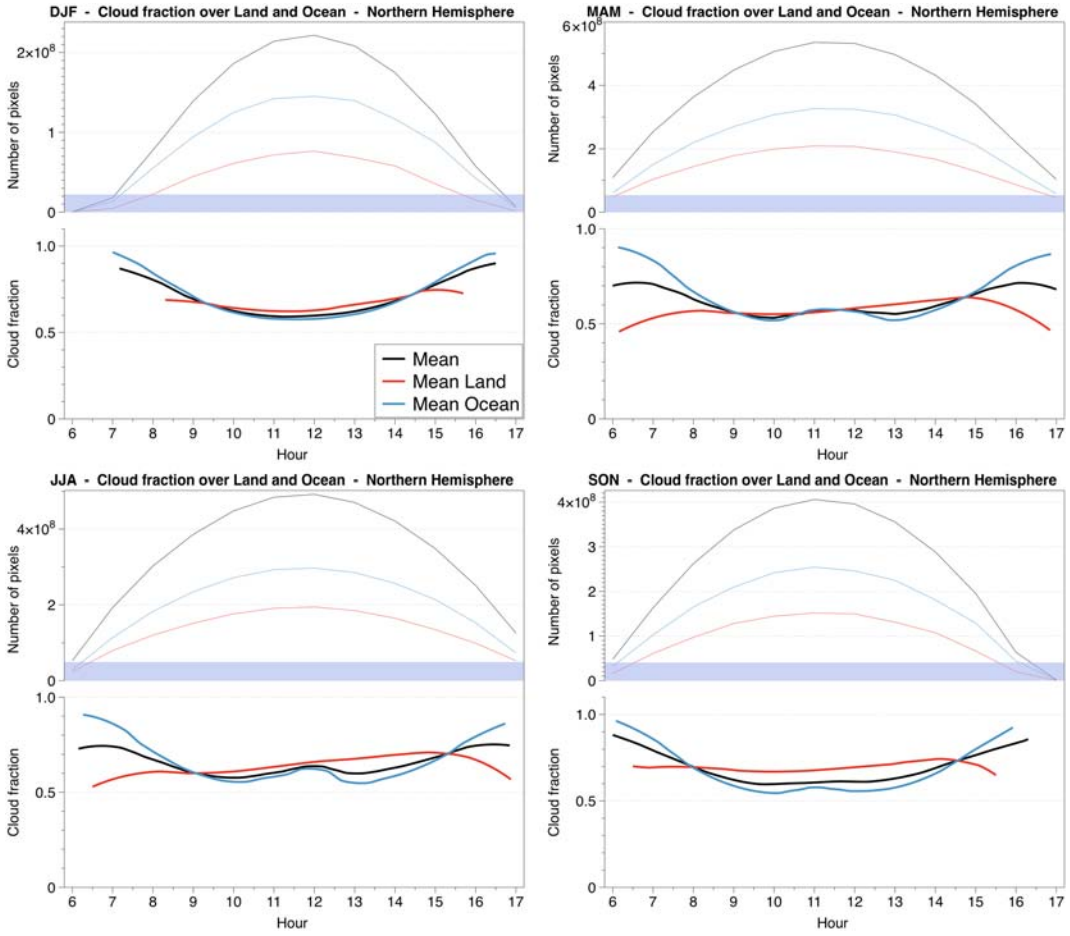

Figure 5. As Figure 4 but for the Northern Hemisphere.

50% in cloud fraction within a day. In contrast, the behavior over land is generally flat with a slight increase in the afternoon. Figure 5 shows the countepart plots for the Northern Hemisphere.

As the majority of our planet is covered by ocean, it is not surprising that the mean behavior of the daytime cloud pattern is closer to the ocean situation, as seen in the black lines of Figures 4 and 5.

Sunglint can cause a slight cloud identification artifact in the EPIC data (Yang et al., 2019). During DJF and MAM, the sunglint areas are located in the Southern Hemisphere and during JJA and SON in the Northern Hemisphere (Marshak et al., 2017). The slight increase in cloud fraction at 11 a.m. and 12 p.m. over ocean in Figures 4 (SON and DJF) and 5 (MAM and JJA) is due to retrieval artifacts; the behavior without these effects would be convex, as it is during the other seasons.

3.3. Effect of VZA

Previous calculations of cloud fraction with EPIC provided values in agreement with other instruments, showing differences of only 1.5% in the global cloud fraction compared to a GEO-LEO composite data set (Yang et al., 2019). This section assesses the effect of the VZA over land and ocean. Due to EPIC's vantage point, the size of a pixel increases as $\cos^{-1}$(VZA). Since VZA and SZA are almost the same for EPIC (4° to 12° difference between VZA and SZA; see Marshak et al., 2018), it is possible to study the effect of the VZA using the SZA information field contained in the granules.

We will consider only pixels within a certain range of SZA. For example, pixels with SZA = 60° are approximately twice the size of the central pixels of the image, and only 4% of pixels have SZA larger than 78° (Yang

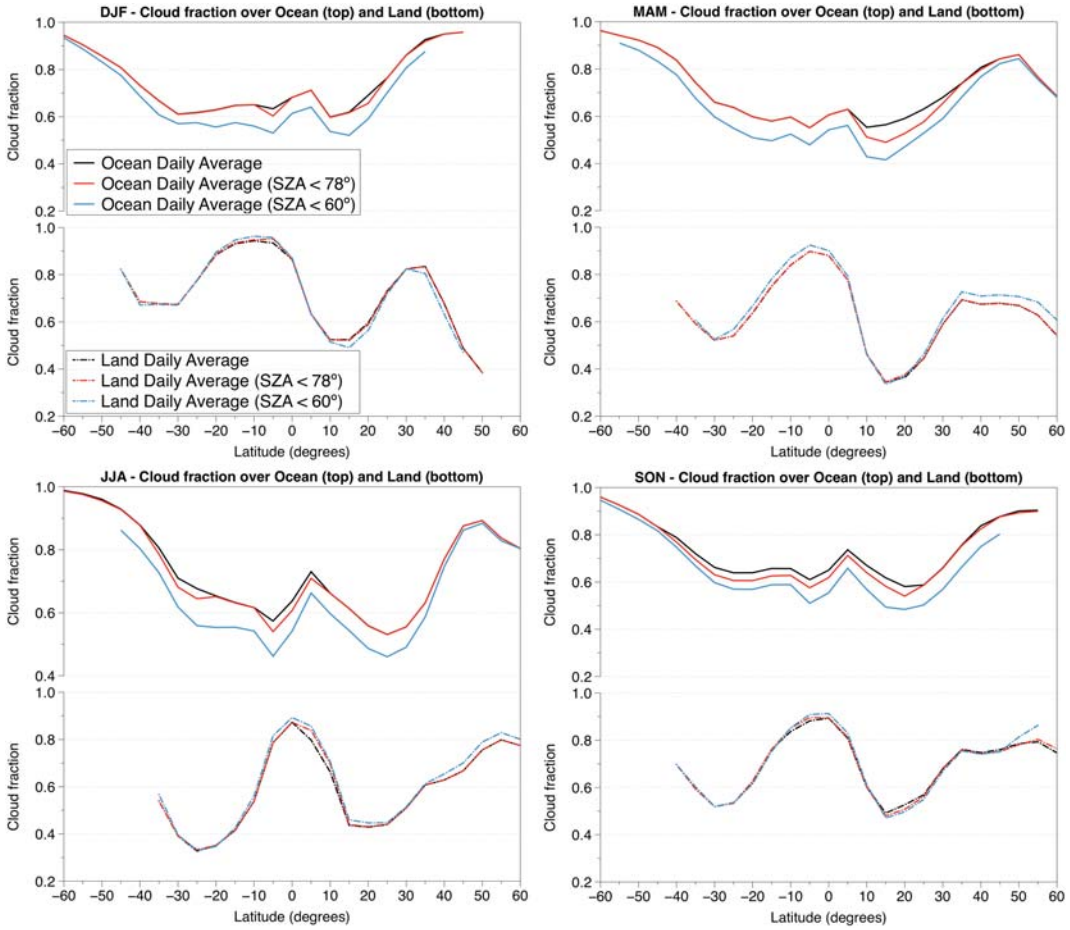

Figure 6. Effect of SZA on daytime average over ocean (top panels) and over land (bottom panels) for four seasons, considering all pixels (black lines), only those pixels with SZA < 78° (red lines) and SZA < 60° (blue lines).

et al., 2018). As larger pixels have a higher probability to be classified as cloudy, we will study different situations to observe the main effects of SZA.

Figure 6 shows the latitudinal behavior of the daytime average for the different seasons when we consider all pixels (black lines), only those with SZA < 78° (red lines) and only those with SZA < 60° (blue lines), separating between land (bottom) and ocean (top).

In general, we observe that the effect of not considering low Sun over ocean (top) leads to a decrease in the daytime average values, while over land (bottom) the variations are much smaller (if any). The observed drop in cloud fraction over land in latitudes around 10° is explained by the absence of clouds over the Sahara desert, as illustrated in the EPIC example image shown in the left panel of Figure 1.

In Figure 7, we analyze the hourly behavior over ocean in detail for the whole globe, considering all pixels (black line), only those pixels with SZA < 78° (red line) and with SZA < 60° (blue line). Generally, the limitation of the SZA only affects the early morning and late afternoon data. As only about 4% of the pixels have SZA higher than 78°, the results including all pixels or only those with SZA < 78° are very close. When we extend the restriction to SZA < 60°, the cloud fraction maintains the characteristic convex shape over ocean in all seasons, although the values slightly decrease in general. On the other hand, as seen in Figure 8, the behavior over land is generally flat with a very slight increase in the afternoon. When restricting the SZA < 60°, we observe a divergence from the general behavior during early morning and late afternoon for some seasons; we may be excluding specific regions that tend to have a lower cloud fraction than the average.

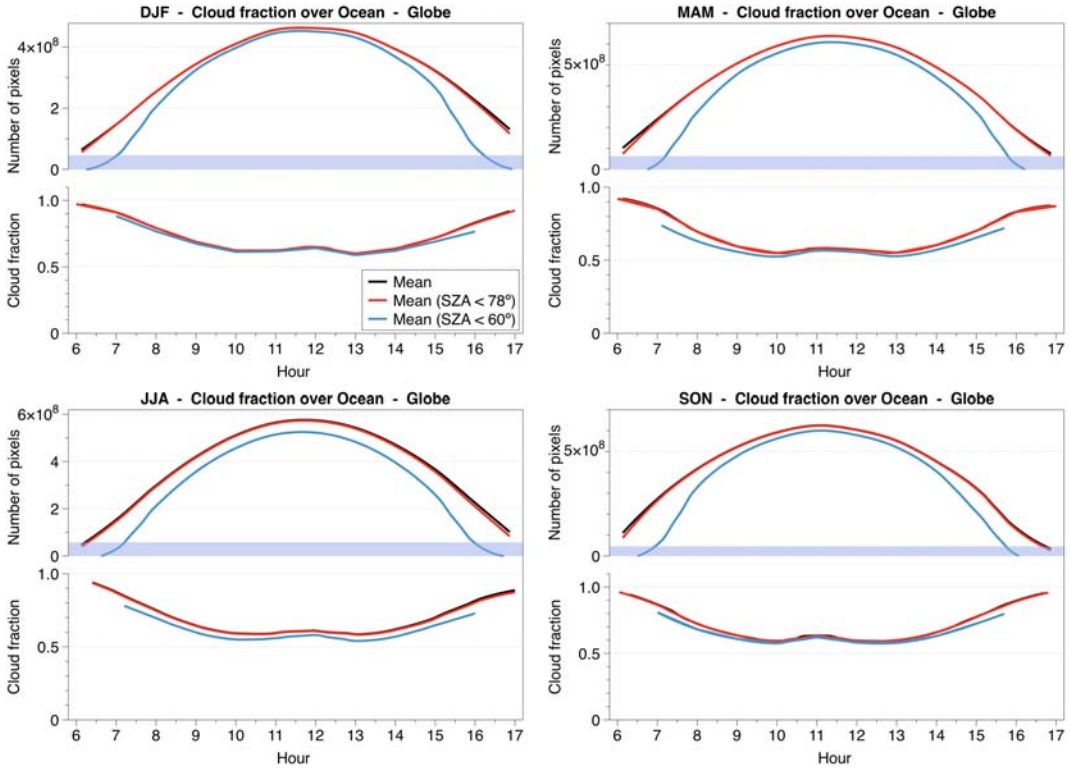

Figure 7. Diurnal variation of global cloud fraction over ocean for the four seasons with different restrictions on the solar zenith angle.

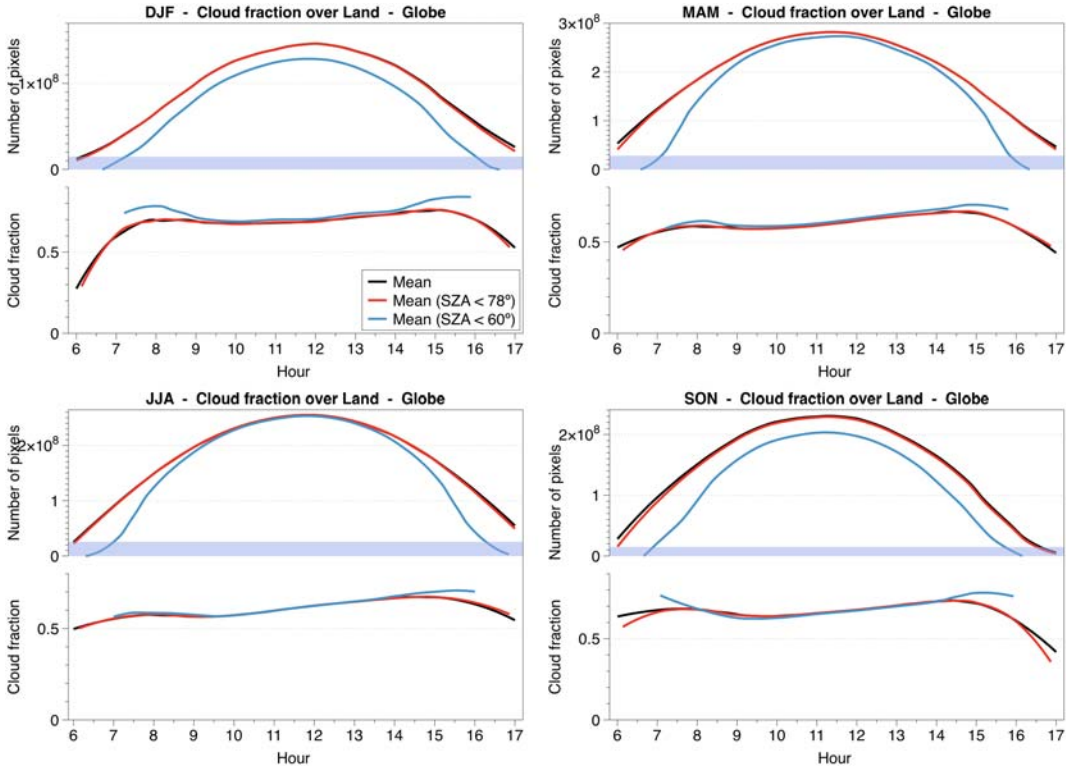

Figure 8. As Figure 7 but for ocean.

4. Conclusions

The special location of DSCOVR at the L1 Lagrangian point allows EPIC to take images of the whole sunlit side of the Earth, capturing different local times from sunrise to sunset every 1 or 2 hr.

As the Level 2 cloud products of EPIC granules include information about cloud mask, geolocation of each pixel and SZA, we were able to study the diurnal cycle of cloud fraction using granules from June 2015 to June 2019. Aggregating those 4 years of data, we were able to study the global cloud fraction variations in time and space for each season.

Although this work mainly focuses on global features, EPIC allows us to also observe the diurnal character of regional features like the Intertropical Convergence Zone. As EPIC captures several images per day, it is useful to track the hourly evolution of short-term features such as volcanic eruptions (Carn et al., 2018) or regional daytime cycles such as marine stratocumulus (Wood, 2012) and convective clouds over land (Yang & Slingo, 2001). The analyses of regional features over the coast of Chile and Baja California and over land in Central Africa and Brazil are included in the supporting information. For marine stratocumulus, our results are compared with Wood (2012) for summertime. Our results show a daytime evolution with larger cloud fraction in the morning, with a minimum around 2–3 p.m., and increasing again in the afternoon. Qualitatively, this shape matches exactly the one presented by Wood (2012) for stratocumulus at these latitudes.

Quantitatively, EPIC shows higher values of cloud fraction than those reported by Wood (2012): They are up to almost 1.0 in the morning instead of 0.75 and with a variability of up to 40% instead of 15% during the day. Note that the calculations used different sensors. EPIC does not have any IR channels, and the cloud mask is based on its observations at the ultraviolet (UV); visible and oxygen A- and B-band wavelengths, and therefore quantitative differences should be expected. Furthermore, EPIC captures the state of the Earth every 1 or 2 hr, while the results of Wood (2012) are based on ISCPP with a frequency of 3 hr.

From the global analysis of the images, we found that, in general, cloud fraction over ocean follows a characteristic convex shape with high values of cloud fraction at early morning and late afternoon. In contrast, when analyzing the diurnal cycle of cloud fraction over land, we do not observe a convex shape and the behavior is almost flat with a slight increase in the afternoon; albeit the exact shape of the diurnal change depends on latitude.

Even though EPIC's cloud mask has been validated before (Yang et al., 2019), as the size of the pixels increases with the VZA, those retrieval artifacts might be influencing the results and providing values of cloud fraction higher than expected. In order to account for that possibility and separate it from physical behavior, we studied cloud fraction changes under different restrictions of the SZA (equivalent to VZA in the case of EPIC). We found that the convex shape over ocean is maintained even for the smaller, more reliable, SZAs, and the behavior over land retains its flat shape during the day.

Acknowledgments
Alfonso Delgado-Bonal's research was supported by the NASA Postdoctoral Program at NASA Goddard Space Flight Center, administered by Universities Space Research Association under contract with NASA, and DSCOVR Science Management project. Lazaros Oreopoulos acknowledges support from NASA's MEASURES, PMM, and CloudSat/CALIPSO Science Team Programs. Yuekui Yang would like to acknowledge funding support from the NASA DSCOVR Science Team Program. Alexander Marshak acknowledges support from NASA's DSCOVR Science Management project. The data sets used in this investigation are available at the NASA's Atmospheric Science Data Center (ASDC), located in the Science Directorate at the NASA'S Langley Research Center in Hampton, Virginia, searching for the DSCOVR EPIC Cloud Products (https://earthdata.nasa.gov/eosdis/daacs/asdc). EPIC images are accessible online (https://epic.gsfc.nasa.gov).

References

Bergman, J. W., & Salby, M. L. (1996). Diurnal variations of cloud cover and their relationship to climatological conditions. *Journal of Climate*, *9*, 2802–2820.

Cairns, B. (1995). Diurnal variations of cloud from ISCCP data. *Atmospheric Research*, *37*, 133–246.

Carn, S. A., Krotkov, N. A., Fisher, B. L., Li, C., & Prata, A. J. (2018). First observations of volcanic eruption clouds from the L1 Earth-Sun Lagrange point by DSCOVR/EPIC. *Geophysical Research Letters*, *45*, 456–464. https://doi.org/10.1029/2018GL079808

Geogdzhayev, I. V., & Marshak, A. (2018). Calibration of the DSCOVR EPIC visible and NIR channels using MODIS Terra and Aqua data and EPIC lunar observations. *Atmospheric Measurement Techniques*, *11*, 359–368.

ISLSCP, Jet Propulsion Laboratory (2013). ISLSCP II land and water masks with ancillary data. Data set. Available on-line [http://daac.ornl.gov/] from Oak Ridge National Laboratory Distributed Active Archive Center, Oak Ridge, Tennessee, USA.

King, M. D., Platnick, S., Menzel, W. P., Ackerman, S. A., & Hubanks, P. A. (2013). Spatial and temporal distribution of clouds observed by MODIS onboard the Terra and Aqua satellites. *IEEE Transactions on Geoscience and Remote Sensing*, *51*(7), 3826–3852.

Kondragunta, C. R., & Gruber, A. (1994). Diurnal variation of the ISCCP cloudiness. *Geophysical Research Letters*, *21*(18), 2015–2018.

Levy, R. C., Mattoo, S., Sawyer, V., Shi, Y., Colarco, P. R., Lyapustin, A. I., et al. (2018). Exploring systematic offsets between aerosol products from the two MODIS sensors. *Atmospheric Measurement Techniques*, *11*, 4073–4092.

Loeb, N. G., & Doelling, D. R. (2020). CERES Energy Balanced and Filled (EBAF) from Afternoon-Only Satellite Orbits. *Remote Sensing*, *12*(8), 1280. https://doi.org/10.3390/rs12081280

Marshak, A., Herman, J., Szabo, A., Carn, S., Cede, A., Geogdzhayev, I., et al. (2018). Earth observations from DSCOVR/EPIC instrument. *Bulletin of the American Meteorological Society*, *99*(9), 1829–1850. https://doi.org/10.1175/BAMS-D-17-0223.1

Marshak, A., Várnai, T., & Kostinski, A. (2017). Terrestrial glint seen from deep space: Oriented ice crystals detected from the Lagrangian point. *Geophysical Research Letters*, *44*, 5197–5202. https://doi.org/10.1002/2017GL073248

Platnick, S. E., Meyer, K. G., King, M. D., Wind, G., Amarasinghe, N., Marchant, B., et al. (2017). The MODIS cloud optical and microphysical products: Collection 6 updates and examples from Terra and Aqua. *IEEE Transactions on Geoscience and Remote Sensing*, *55*(1), 502–525. https://doi.org/10.1109/TGRS.2016.2610522

Rossow, W. B., & Schiffer, R. A. (1991). ISCCP cloud data products. *Bulletin of the American Meteorological Society*, *71*, 2–20.

Wild, M., Folini, D., Hakuba, M. Z., Schär, C., Seneviratne, S. I., Kato, S., et al. (2015). The energy balance over land and oceans: An assessment based on direct observations and CMIP5 climate models. *Climate Dynamics*, *44*, 3393–3429.

Wood, R. (2012). Stratocumulus clouds. *Monthly Weather Review*, *140*, 2373–2423.

Yang, G.-Y., & Slingo, J. (2001). The diurnal cycle in the tropics. *Monthly Weather Review*, *129*, 784–801.

Yang, W., Marshak, A., Várnai, T., & Knyazikhin, Y. (2018). EPIC spectral observations of variability in Earth's global reflectance. *Remote Sensing*, *10*(2), 254. https://doi.org/10.3390/rs10020254

Yang, Y., Meyer, K., Wind, G., Zhou, Y., Marshak, A., Platnick, S., et al. (2019). Cloud products from the Earth Polychromatic Imaging Camera (EPIC): Algorithms and initial evaluation. *Atmospheric Measurement Techniques*, *12*(3), 2019–2031. https://doi.org/10.5194/amt-12-2019-2019

Yin, J., & Porporato, A. (2017). Diurnal cloud cycle biases in climate models. *Nature Communications*, *8*, 2269.

Young, A. H., Knapp, K. R., Inamdar, A., Hankins, W., & Rossow, W. B. (2018). The international satellite cloud climatology project H-series climate data record product. *Earth System Science Data*, *10*, 583–593.